Inferring Spatial Interface Dependencies from Co-change Records in Civil Infrastructure Design Models

Ryoko Arashida[1] and Masahide Horita[2]

[1] Institute of Engineering Innovation, School of Engineering, The University of Tokyo, Tokyo, Japan
[2] Department of Civil Engineering, School of Engineering, The University of Tokyo, Tokyo, Japan
arashida@i-con.t.u-tokyo.ac.jp, horita@g.ecc.u-tokyo.ac.jp

Abstract

This paper presents a data-driven framework for inferring spatial interface dependencies in large-scale civil infrastructure design using empirically observed co-change as a proxy for coordination-related interactions. Using tender and as-built 3D models from an expressway project, object-level changes are identified and distance-based inter-category features are constructed to predict change occurrence. Among the evaluated classifiers, LightGBM achieved the best performance (average G-mean = 0.903). The results show that co-change is better explained by neighborhood-level spatial interactions than by single nearest-neighbor relationships. Distance cutoff analysis indicates that predictive performance saturates within limited spatial ranges, typically within about 30 m in this dataset. Furthermore, Individual Conditional Expectation (ICE) analysis reveals five distinct distance-dependent co-change patterns, while also identifying cases where distance reflects broader spatial heterogeneity rather than direct interface relationships. These findings suggest that spatial distance captures a substantial portion of co-change behavior and can support prioritization of interface checks and selection of search radii in infrastructure design coordination.

Keywords –

Co-change; Hard/soft clash; Building Information Modeling; Machine learning; Design change; Change Propagation

1 Introduction and Related Works

In large-scale Architecture, Engineering, and Construction (AEC) projects, resolving all inconsistencies during design is unrealistic because design and construction are separated, site conditions are uncertain, and production is largely project-specific [1, 2]. Consequently, design changes are unavoidable and are major drivers of cost overruns and schedule delays [3, 4]. The key challenge is therefore not to eliminate changes, but to clarify when they propagate across elements and to limit cascading coordination efforts.

Change propagation is governed by interface constraints between elements, particularly geometric relationships such as connectivity, proximity, and clearance [5]. Under these constraints, local modifications often require adjustments to related elements, which are observed as coordinated updates among multiple components. In this study, such coordinated updates are referred to as co-change.

In software engineering, several studies have analyzed version histories to identify software artifacts that tend to be modified together, often described as logical coupling, evolutionary coupling, or change patterns [6–8]. However, these studies primarily focus on temporal co-change relationships in software repositories and do not explicitly consider spatial relationships between physical components. In contrast, spatial dependencies are central in civil infrastructure systems and are explicitly addressed in this study through geometric distance-based analysis.

With the widespread adoption of Building Information Modeling (BIM), automated detection of interface-related inconsistencies has become widely used. Model-checking research has expanded from hard/soft clash detection to workspace conflicts in construction planning [9–11], and compliance checking against regulations and design rules [12–14]. However, these approaches depend on explicitly specified constraints and dependency rules, making large-scale deployment costly to develop and maintain. Even soft clash detection often requires clearance rules for each object pair, which is burdensome in practice [15].

In parallel, computer graphics and geometric learning have developed methods to extract implicit geometric relationships from large shape collections by learning regularities in component arrangements and encoding them as reusable knowledge or constraints [16–20]. However, these approaches typically assume stable component decompositions and limited interaction ranges, limiting their applicability to the AEC domain. While ML-based generative design has been actively studied in AEC using drawings and photographs, existing work largely focuses on early-stage, single-building problems and does not adequately capture relationships among heterogeneous elements, due to the knowledge- and reasoning-intensive nature of AEC design [21].

These limitations motivate the use of co-change as an empirical signal for inferring interface dependencies. By treating change records as observable outcomes of coordination processes, spatial relationships between elements can be analyzed without explicitly defining all interface rules.

In this study, object-level changes **derived** from differences between tender and as-built models are used to analyze co-change among structural categories and its dependence on object-to-object distance. **Focusing** on geometric interface **conditions, distance**–co-change relationships are identified and organized into interpretable patterns using Individual Conditional Expectation (ICE) analysis.

2 Methodology

2.1 Workflow Overview

Figure 1 illustrates the workflow of this study. The inputs are the tender and as-built models of an expressway infrastructure project. As a preprocessing step, both models are segmented into category-specific analysis objects using predefined rules, and each object is assigned a binary change label indicating whether it has changed between the two models.

Based on these labeled objects, spatial interfaces between categories are represented using distance-based features. Specifically, multiple inter-category distance representations are constructed to characterize the spatial relationship between a target object and potentially related objects in other categories. These distance-based representations serve as explanatory variables for predicting object-level change occurrence.

The analysis proceeds in four stages. First, a suitable classification model is selected through comparative evaluation. Second, alternative distance-feature representations are assessed to examine how spatial information should be encoded. Third, effective distance cutoffs are determined to identify the spatial ranges within which distance information contributes meaningfully to change prediction. Fourth, important distance features are identified through feature selection to obtain a compact and informative representation.

For the selected distance features, Individual Conditional Expectation (ICE) is employed to examine how changes in distance are associated with changes in predicted change probability. By jointly interpreting the shapes of the mean ICE curves and the corresponding distance distributions, co-change behavior between categories is organized into interpretable interface patterns.

The outputs of the framework are (1) effective distance ranges for predicting change occurrence in each target category and (2) a typology of distance-dependent, interface-based co-change patterns.

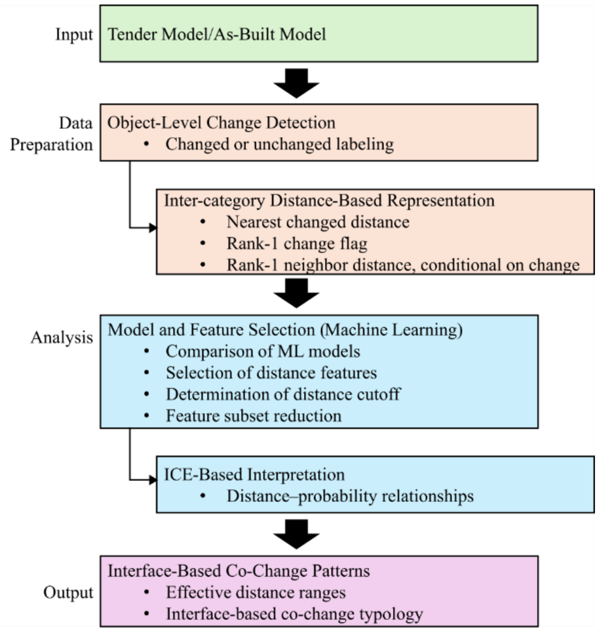

Figure 1. Overview of the proposed analysis framework.

2.2 Data and Preprocessing

2.2.1 Target Models, Categories, and Object Segmentation

The dataset comprises the tender and as-built models of an expressway infrastructure project. The study area covers approximately 350 m × 2100 m and includes bridge and embankment sections, excluding cut sections and tunnels. A total of 25 design categories are analyzed.

Because civil infrastructure models often include large continuous elements whose native BIM representations do not correspond to analysis units, category-specific segmentation rules were defined to obtain consistent object-level units reflecting structural boundaries and management units. Continuous elements were segmented based on structural or alignment-based rules. For bridge-related categories, segmentation followed structural boundaries, while for road and earthwork categories, objects were segmented along the road centerline at 20 m intervals, corresponding to the cross-section spacing in the tender drawings. In contrast, discrete components were treated as single elements without further subdivision. Table 1 summarizes the category definitions and sample sizes, and Figure 2 illustrates the bridge segmentation scheme.

Table 1. Summary of categories, sample sizes, and change rates.

Category	Sample Size	Change Rate
Expressway Pavement	**317**	**21%**
Service Road Pavement	93	95%
Earthwork Crest	38	26%
Earthwork Toe	41	49%
Deck Slab	**1,343**	**35%**
Main Girder	1,356	96%
Cross Girder	**1,332**	**30%**
Pier Shaft	107	3%
Pier Cap	66	5%
Foundation	70	4%
Bearing	199	2%
Bearing Pedestal	199	6%
Fall Protection	20	70%
Barrier Wall	**2,874**	**28%**
Bridge Inspection Walkway	93	99%
Bridge Drainage	100	89%
Detention Pond	11	100%
Drainage	**848**	**40%**
Temporary Support	207	99%
Construction Yard	75	28%
Girder Storage	401	100%
Crane Position	170	100%
Access Road	65	9%
River Diversion	7	100%

Note: Categories shown in **bold** indicate the target categories selected for analysis (Section 2.3).

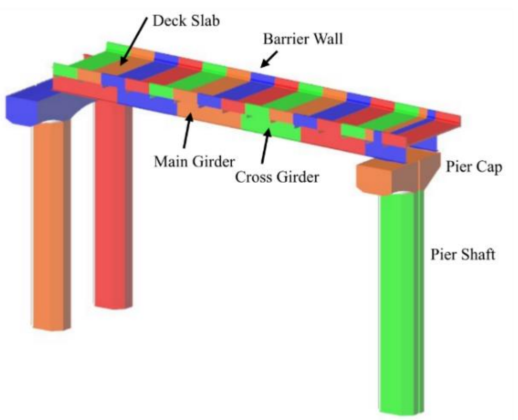

Figure 2. Example of object segmentation for bridge components.

2.2.2 Definition of Change Occurrence

Objects from the tender and as-built models are matched at the object level after projecting their coordinates onto a common 2D plane. An object is labeled as changed if (1) it appears in only one model, or (2) if present in both models, its centroid displacement is at least 10 cm. All remaining objects are labeled as unchanged.

The 10 cm threshold is used as a practical tolerance to mitigate minor positional noise introduced during model creation and integration while preserving substantively meaningful changes. Category-wise change rates are reported in Table 1.

2.3 Target Category Selection

Among the 25 categories, only categories that meet the following criteria are analyzed to ensure stable model training and interpretable results: at least 240 objects in the tender model and a change rate between 20% and 80%. For each target category, distance features are constructed using the other 24 categories as predictor sources. The minimum sample size of 240 was set as ten times the number of explanatory categories, and the change-rate range was used to avoid severe class imbalance that can destabilize the classifier and obscure distance–change relationships. Consequently, although only a subset of categories is used as prediction targets, all categories are retained as sources of explanatory distance features, meaning that their spatial influence on the analyzed targets remains represented in the model.

Based on Table 1, five categories satisfy these criteria: expressway pavement, deck slab, cross girder, barrier wall, and drainage.

2.4 Distance-Feature Construction

For each object in each of the five target categories, neighboring objects are extracted from all other categories. All objects are projected onto a common 2D plane prior to distance computation. In civil infrastructure models, most design categories occupy relatively consistent vertical bands (e.g., road-surface elements versus ground-level components). As a result, situations in which objects appear close in plan view but are vertically separated tend to occur systematically between specific category pairs rather than randomly at the object level. Because the model uses category-based distance features, such systematic vertical offsets are reflected consistently in the learned relationships rather than introducing random noise. To partially account for vertical structure, Earthwork and Pier categories were subdivided into two components each, representing distinct interaction zones even when distances are computed on a 2D projection.

For each target object and each non-target category, 50 candidate neighbors are first identified based on centroid distances. Exact boundary-based distances are then computed on the 2D plane, and the 20 closest neighbors are retained together with their distances and change labels.

For each target category, four datasets are constructed using distance-based features derived from other categories. If no changed object is found within the 20 nearest neighbors, a sentinel value (maximum observed distance + 10 m) is assigned. This value is intentionally placed beyond the range of typical neighbor distances so that it functions as an indicator of “no nearby change” rather than a meaningful spatial distance, and therefore does not affect the learned splits of the classifier. The datasets differ in how distance information is represented:

- Dataset 1: the minimum distance to the nearest changed object in each category.
- Dataset 2: a binary indicator of whether the nearest neighbor (rank 1) is changed.
- Dataset 3: distance to the nearest neighbor, conditional on that neighbor being changed.
- Dataset 4: all features from Datasets 1–3 combined.

To assess whether nearest-neighbor relationships alone can capture design coordination effects, the rank-1 datasets (Datasets 2 and 3) are compared with Dataset 1, which can capture changed neighbors beyond the nearest object.

2.5 Machine Learning (ML) Setup for Change Prediction

For each target category, the prediction models use the change label of the target object as the response variable, while the distance-based features derived from the remaining categories (Datasets 1–4) are used as explanatory variables. Change prediction is formulated as a binary classification task, in which each object is labeled as either changed or unchanged. The following algorithms are compared:

- Logistic regression (L1/L2/elastic net)
- Random Forest
- Extra Trees
- HistGradientBoosting
- LightGBM

All models are implemented in Python using scikit-learn and LightGBM with default hyperparameters. For each target category, the data are split into 90% for training and 10% for testing. This procedure is repeated for 10 different random seeds, and evaluation metrics are averaged across seeds to improve robustness and reproducibility. To account for class imbalance, performance is evaluated primarily using the G-mean, defined as the geometric mean of sensitivity and specificity.

2.6 Distance Cutoff, Feature Selection, and ICE-Based Patterning

A distance cutoff sensitivity analysis is performed to identify the spatial range over which distance features contribute to explaining co-change. An upper distance limit is imposed on all features and progressively reduced, while classification performance is evaluated. Distances exceeding the limit are replaced with a large value, and the effective cutoff is defined as the smallest limit that retains at least 95% of the baseline performance.

Feature selection is then conducted using the selected ML model. Features are ranked by LightGBM gain and added sequentially while monitoring performance. The final feature set is defined as the smallest set that retains at least 95% of the baseline performance.

ICE is then computed for each target category and each retained distance feature using models retrained on the final feature set. For each feature, object-level ICE curves and their mean are derived to characterize the distance–change probability relationship. ICE is evaluated from 0 m to the effective distance cutoff or the maximum observed distance, whichever is smaller.

To stabilize estimation, distances are discretized into 30 equal-width bins. Bins with fewer than five samples are excluded, and features with fewer than three valid bins are removed as unreliable. In addition, ICE curves with less than 1% probability variation are excluded, as they indicate negligible sensitivity to distance. Such low-variation curves correspond to nearly flat relationships and primarily introduce noise rather than additional pattern types.

Co-change interface patterns are identified from the mean ICE curves and their associated distance distributions. Classification considers both the shape of the ICE curves (e.g., monotonic, plateau, or peak behavior) and the distribution of observed distances, and category pairs are grouped into patterns exhibiting similar distance-dependent behavior.

3 Results

3.1 Comparison of Classification Algorithms

Across all target categories and dataset settings, LightGBM achieved the highest mean G-mean (0.903) and showed stable performance across random seeds. Although performance varied by category, LightGBM generally maintained G-mean ≥ 0.80 and was selected for subsequent analyses.

3.2 Comparison of Feature Representations and Dataset Selection

Using LightGBM, Dataset 4 yielded the best overall performance, while Dataset 1 achieved a comparable G-mean with substantially fewer features. As shown in Figure 3, Dataset 1 provided a stable and interpretable baseline across target categories, whereas Datasets 2 and 3 exhibited greater variability. Therefore, Dataset 1 was adopted for subsequent analyses. The baseline G-mean values with Dataset 1 were 0.817 (expressway pavement), 0.938 (deck slab), 0.942 (cross girder), 0.978 (barrier wall), and 0.889 (drainage).

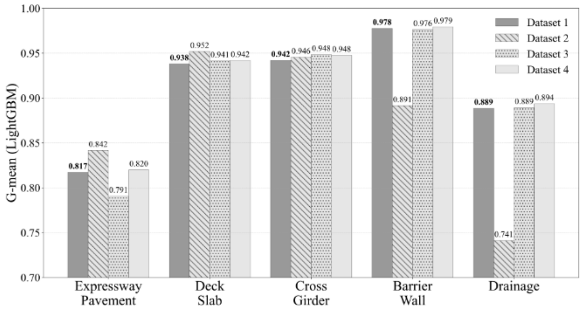

Figure 3. Comparison of distance-based feature representations using G-mean (LightGBM).

3.3 Effective Distance Ranges

Distance cutoff sensitivity analysis indicated that performance improvements saturated within a limited spatial range for most target categories. The resulting effective distance cutoffs (defined in Section 2.6) differed by category and are summarized in Figure 4: 15.5 m (expressway pavement), 0.5 m (deck slab), 0.5 m (cross girder), 2.0 m (barrier wall), and 28.5 m (drainage).

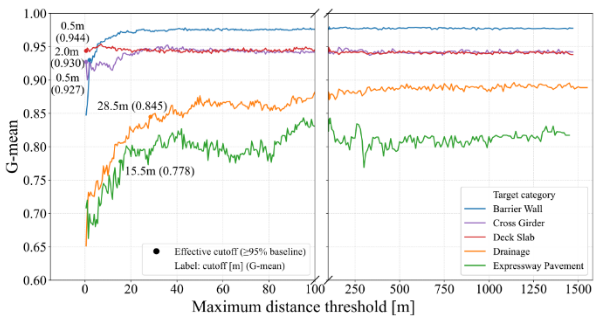

Figure 4. Distance Cutoff Sensitivity of G-mean Performance.

3.4 Important Features

Gain-based feature selection produced compact feature sets while retaining at least 95% of the baseline performance. The retained distance features are:

- Expressway Pavement (8): Barrier Wall, Girder Storage, Deck Slab, Crane Position, Earthwork Toe, Service Road Pavement, Fall Protection, Drainage
- Deck Slab (1): Cross Girder
- Cross Girder (1): Deck Slab
- Barrier Wall (4): Cross Girder, Deck Slab, Main Girder, Service Road Pavement
- Drainage (6): Detention Pond, Expressway Pavement, Service Road Pavement, Earthwork Toe, Earthwork Crest, Temporary Support

3.5 ICE Patterns of Distance-Dependent Co-Change Behavior

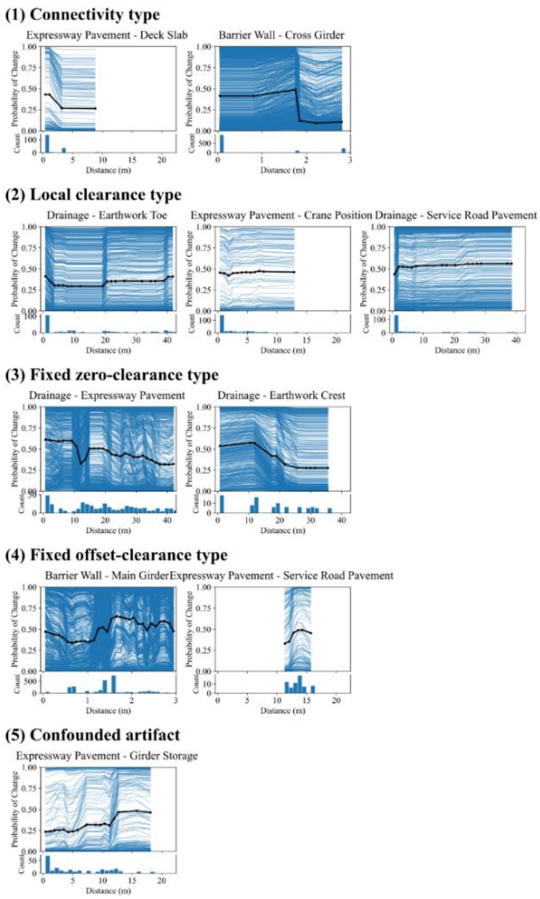

Figure 5. Classification of distance-based co-change interface patterns based on ICE analysis.
Note: Blue lines show individual ICE curves, the black line indicates their mean ICE curve, and the histogram shows the distance distribution.

ICE analysis was applied to the features remaining after feature selection and reliability filtering, leaving only 10 category-pair distance features overall. Figure 5 presents the corresponding mean ICE curves and distance histograms. Following the criteria in Section 2.6, these profiles were grouped into five co-change interface patterns, reflecting differences in the mean ICE shapes and associated distance distributions.

4 Discussion

4.1 Implications Beyond the Nearest Neighbor

Across the evaluated representations, Dataset 1, which uses the minimum distance to the nearest changed object in each category, provided higher performance and greater stability than Datasets 2 and 3, which rely on the change state of the single nearest neighbor (Figure 3). This indicates that co-change is not explained solely by the nearest object, but is more strongly associated with the presence of changed objects within a local neighborhood. These results suggest that spatial distance captures a substantial portion of the observed co-change behavior, highlighting spatial proximity as a key predictive signal for interface dependencies.

4.2 Implications of Effective Distance Upper Bounds

Distance cutoff sensitivity analysis showed that predictive performance was largely preserved as information from more distant objects was excluded, with performance generally saturating within approximately 30 m (Figure 4). This supports the view that coordination is primarily governed by local spatial interactions. However, the effective distance ranges varied across categories, indicating that a uniform threshold may be suboptimal and that category-specific search radii could provide a more rational basis for practical checks. In particular, categories with higher predictive accuracy were dominated by short-distance information, whereas lower-accuracy categories exhibited broader effective ranges, suggesting a greater influence of longer-range spatial constraints.

4.3 Differences in the Number of Important Features and Dependency Complexity

As shown in Section 3.4, some target categories preserved predictive performance using only a small set of distance features, suggesting that their change occurrence is strongly driven by a limited number of distinct interface relationships. In contrast, categories with lower predictive accuracy, particularly expressway pavement and drainage, required a larger set of important features, indicating more multifaceted dependencies on surrounding categories and/or the influence of factors not fully captured by distance features alone.

4.4 Interpretation of ICE-Based Patterns and Mechanism Hypotheses

As illustrated in Figure 5, ICE profiles of the important distance pairs can be grouped into five types, reflecting distinct ways in which distance is associated with co-change. Here, ICE refers to the mean ICE profile, and DD denotes the corresponding distance distribution.

1. Connectivity type (ICE: sharp drop after peak; DD: concentrated near zero)

High co-change probability at near-zero distances followed by a rapid decline suggests direct or near-contact interfaces, where coordination is driven by maintaining compatibility at connection points.

2. Local clearance type (ICE: plateau; DD: zero-peaked but widespread)

A flat ICE profile despite broad distance distributions indicates that effective clearance varies across objects, implying that uniform category-level rules may be insufficient.

3. Fixed zero-clearance type (ICE: gradual decay after peak; DD: zero-peaked and widespread)

A gradual decrease in co-change probability with distance suggests proximity-driven interactions without strict clearance requirements, primarily reflecting avoidance of hard clashes.

4. Fixed offset-clearance type (ICE: increase before peak, gradual decay after peak; DD: non-zero peak and widespread)

A peak at non-zero distances indicates characteristic clearance bands, consistent with standardized layouts or design rules.

5. Confounded artifact (non-mechanistic; reported for completeness)

Anomalous patterns driven by project-specific spatial heterogeneity rather than direct interface mechanisms are excluded from the primary typology.

4.5 Transferability and Prospective Use

The present results are derived from a single expressway project and should not be interpreted as universally transferable numerical rules. In particular, absolute distance cutoffs and detailed category-pair behaviors may remain partly project-dependent, reflecting the geometry, segmentation scheme, and revision history of the analyzed case.

However, the observed co-change relationships are unlikely to be entirely project-specific. Many spatial interfaces in civil infrastructure are governed by stable engineering conditions, such as structural connectivity, standard cross-sections, and clearance requirements, which are typically defined by design codes and common practices. As a result, while numerical thresholds may vary, the identified interface-pattern types and their spatial tendencies are expected to generalize across comparable projects.

The framework can therefore be used to extract reusable coordination knowledge from completed projects. Patterns identified from historical revisions can inform subsequent projects by suggesting category pairs requiring closer coordination and by providing initial search ranges for spatial checks.

Transferability is expected to be highest among projects sharing similar asset types and regulatory environments, such as highway projects designed under comparable design codes and maintenance requirements. By contrast, application to substantially different infrastructure types (e.g., tunnels or coastal structures) or to projects developed under different national or organizational design regimes would require additional empirical data and revalidation.

5 Conclusion

This study proposed a data-driven framework to infer interface dependencies in a large-scale civil infrastructure project using empirically observed co-change events. Object-level changes between tender and as-built models were modeled using distance-based inter-category features, and distance–change relationships were interpreted using ICE.

Using the minimum distance to the nearest changed object within each explanatory category yielded higher accuracy than using only the change state of the single nearest neighbor, indicating that co-change is not adequately explained by one-to-one proximity, and is better characterized at the local neighborhood level. These results also indicate that spatial distance alone captures a substantial portion of the observed co-change behavior. Distance cutoff analysis further showed that most predictive power was retained within category-specific spatial ranges, generally saturating within about 30 m, supporting the use of category-dependent search radii rather than a uniform threshold. In addition, gain-based selection reduced the feature set while retaining at least 95% of baseline performance, and ICE analysis of the retained features revealed five distance-dependent co-change interface patterns, with confounded cases reported separately.

Taken together, these results suggest that the workflow can support the inference of plausible interface-related coordination mechanisms by identifying influential category pairs, the spatial ranges over which distance is informative, and characteristic distance–probability profiles. These outputs provide actionable guidance for prioritizing inter-category checks and designing distance-based search and coordination rules.

It is important to note that the numerical cutoffs and category-pair relationships identified in this study should be interpreted as case-grounded observations rather than universally applicable interface rules. Because the analysis is based on a single infrastructure project, the exact numerical values may vary depending on project geometry, design standards, and coordination practices. Nevertheless, many spatial interface conditions in civil infrastructure are shaped by recurring engineering requirements, such as structural connectivity, clearance provisions, and operation-and-maintenance needs defined in design standards. As a result, while the precise thresholds may differ across projects, the broader pattern classes and relative spatial tendencies identified in this study are expected to remain informative for similar infrastructure projects governed by comparable design regimes. In this sense, the framework provides a practical workflow through which reusable coordination knowledge can be extracted from completed projects and applied to guide interface analysis in future projects of the same type.

This study has several limitations. First, distances were computed based on 2D projections of object geometries, without considering vertical relationships. Although most infrastructure categories occupy relatively consistent vertical bands and vertically distributed elements were subdivided into separate categories, this projection may still simplify certain three-dimensional relationships. Second, object- or project-specific confounding factors, such as construction sections or work packages, were not incorporated. Third, the available dataset was limited in size, and consequently the typology of distance-based interface relationships remains incomplete. In particular, categories with extremely low or extremely high change rates could not be analyzed as prediction targets in the present dataset, although their interface behaviors may warrant investigation in larger datasets. Fourth, the analysis relied solely on spatial distance information derived from geometric changes in the models. Changes without spatial modifications (e.g., material substitutions or schedule adjustments) are therefore outside the scope of the present analysis and may not be represented in the inferred relationships. Addressing such non-geometric change dependencies would require additional data and modeling approaches beyond the scope of the current framework. Finally, the engineering interpretations assigned to the identified pattern types (e.g., connectivity or clearance relationships) should be regarded as plausible explanations of the observed statistical behaviors rather than formal validation against documented design coordination rules. Further validation through expert assessment and comparison with established design practices would help strengthen the practical interpretation of these patterns.

Future work will address these limitations by expanding the dataset to further develop the typology and by incorporating additional parameters. In particular, beyond spatial distance, semantic information embedded in BIM will be integrated to extract interface relationships that cannot be explained by proximity alone.

Acknowledgements

This work was supported by the i-Construction System Studies Endowed Chair, Faculty of Engineering, The University of Tokyo.

References

[1] J. Freire and L. F. Alarcón. Achieving Lean Design Process: Improvement Methodology. *Journal of Construction Engineering and Management*, 128(3):248–256, 2002.

[2] L. Koskela. *Application of the new production philosophy to construction*, volume 72. Stanford university Stanford, 1992.

[3] C. W. Ibbs. Quantitative Impacts of Project Change: Size Issues. *Journal of Construction Engineering and Management*, 123(3):308–311, 1997.

[4] Y. A. Olawale and M. Sun. Cost and time control of construction projects: inhibiting factors and mitigating measures in practice. *Construction Management and Economics*, 28(5):509–526, 2010.

[5] P. J. Clarkson, C. Simons, and C. Eckert. Predicting Change Propagation in Complex Design. *Journal of Mechanical Design*, 126(5):788–797, 2004.

[6] T. Zimmermann, A. Zeller, P. Weissgerber, and S. Diehl. Mining version histories to guide software changes. *IEEE Transactions on Software Engineering*, 31(6):429–445, 2005.

[7] A. T. T. Ying, G. C. Murphy, R. Ng, and M. C. Chu-Carroll. Predicting source code changes by mining change history. *IEEE Transactions on Software Engineering*, 30(9):574–586, 2004.

[8] H. Gall, K. Hajek, and M. Jazayeri. Detection of logical coupling based on product release history. In *Proceedings. International Conference on Software Maintenance*, pages 190–198, 1998.

[9] A. K. Agrawal, Y. Zou, L. Chen, M. Abdelmegid, V. A. González, and H. Jin. Leveraging linked data for space constraints checking of mobile cranes in modular construction assembly lookahead planning. *Advanced Engineering Informatics*, 68:103778, 2025.

[10] X. Su and H. Cai. Life Cycle Approach to Construction Workspace Modeling and Planning. *Journal of Construction Engineering and Management*, 140(7):04014019, 2014.

[11] M. S. Dashti, M. RezaZadeh, M. Khanzadi, and H. Taghaddos. Integrated BIM-based simulation for automated time-space conflict management in construction projects. *Automation in Construction*, 132:103957, 2021.

[12] P. Pauwels, E. van den Bersselaar, and L. Verhelst. Validation of technical requirements for a BIM model using semantic web technologies. *Advanced Engineering Informatics*, 60:102426, 2024.

[13] R. Wang, D. A. S. Samarasinghe, L. Skelton, and J. O. B. Rotimi. A Study of Design Change Management for Infrastructure Development Projects in New Zealand. *Buildings*, 12(9):1486, 2022.

[14] L. Shi and D. Roman. From Standards and Regulations to Executable Rules: A Case Study in the Building Accessibility Domain. In *CEUR Workshop Proceedings*, 2017.

[15] S. Mehrbod, S. Staub-French, N. Mahyar, and M. Tory. Beyond the clash: investigating BIM-based building design coordination issue representation and resolution. *Journal of Information Technology in Construction*, 24, 2019.

[16] N. Fish, M. Averkiou, O. van Kaick, O. Sorkine-Hornung, D. Cohen-Or, and N. J. Mitra. Meta-representation of shape families. *ACM Trans. Graph.*, 33(4):34:1–11, 2014.

[17] E. Kalogerakis, S. Chaudhuri, D. Koller, and V. Koltun. A probabilistic model for component-based shape synthesis. *ACM Trans. Graph.*, 31(4):55:1–11, 2012.

[18] K. Genova, F. Cole, D. Vlasic, A. Sarna, W. T. Freeman, and T. Funkhouser. Learning Shape Templates With Structured Implicit Functions. In *Proceedings of the IEEE/CVF International Conference on Computer Vision*, pages 7154–7164, 2019.

[19] Z. Chen and H. Zhang. Learning Implicit Fields for Generative Shape Modeling. In *Proceedings of the IEEE/CVF Conference on Computer Vision and Pattern Recognition*, pages 5939–5948, 2019.

[20] M. Kodnongbua, B. Jones, M. B. S. Ahmad, V. Kim, and A. Schulz. ReparamCAD: Zero-shot CAD Re-Parameterization for Interactive Manipulation. In *SIGGRAPH Asia 2023 Conference Papers*, pages 1–12, 2023.

[21] X. Zhuang, P. Zhu, A. Yang, and L. Caldas. Machine learning for generative architectural design: Advancements, opportunities, and challenges. *Automation in Construction*, 174:106129, 2025.